Polymer 50 (2009) 6032–6042

Contents lists available at ScienceDirect

Polymer

journal homepage: www.elsevier.com/locate/polymer

Cross-linked latex particles grafted with polyisoprene as model rubber-compatible fillers

Mario Gauthier*, Abdul Munam

Department of Chemistry, Institute for Polymer Research, University of Waterloo, 200 University Ave. West, Waterloo, ON N2L 3G1, Canada

ARTICLE INFO

Article history:
Received 15 May 2009
Received in revised form
2 October 2009
Accepted 7 October 2009
Available online 28 October 2009

Keywords:
Fillers
Rubber
Core-shell polymers

ABSTRACT

Model filler particles were obtained by grafting polyisoprene (PIP) chains onto spherical latex particles of polystyrene cross-linked with 12 mol% divinylbenzene. These particles, with a narrow size distribution and a diameter of ca. 400 nm, were synthesized by emulsifier-free starved-feed emulsion polymerization. Acetyl coupling sites were introduced randomly at either low (5 mol%) or high (30 mol%) target substitution levels on the latex particles by Friedel–Crafts acylation with acetyl chloride and $AlCl_3$ in nitrobenzene. 'Living' polyisoprenyllithium chains, generated from isoprene and *sec*-butyllithium (*sec*-BuLi), were then coupled with the acetylated particles. The PIP side chains had a high 1,4-polyisoprene microstructure content and a number-average molecular weight (M_n) of either 1.5×10^3 (1.5 K), 5×10^3 (5 K), or 3×10^4 (30 K). The PIP content of the grafted particles was determined from the yield of isolated particles and by ^{1}H NMR spectroscopy analysis. The grafted latex particles were blended in solution with linear polyisoprene ($M_n = 3.95 \times 10^5$, 395 K). The influence of the filler–matrix interactions on the rheological behavior of the blends was determined by dynamic mechanical analysis for the different filler blends. Increases in complex viscosity and storage modulus, and decreased damping factors were observed in all cases relatively to the pure matrix polymer. The enhancements, decreasing in the order 30 mol% > 5 mol% acetylation, and with the grafted PIP chain length as 30 K > 5 K ≈ 1.5 K, are deemed to reflect the extent of interactions between the filler particles and the polymer matrix.

1. Introduction

Commercial plastics and rubbers are often filled with solid particles, either to enhance their mechanical properties or to reduce cost [1]. The properties of these materials depend primarily on the interactions between the matrix and the filler particles, although interparticle interactions are also important [2]. Consequently, the influence of physical interactions on the rheology of filled polymers can be very complex [3,4]. Strong interactions between the matrix polymer and the filler particles can increase the viscosity and the dynamic moduli, for example through adsorption of the polymer on the filler surface restricting chain mobility within the matrix. The nature and surface composition of the particles, as well as matrix properties such as the polarity and the molecular weight influence the rheology of the mixtures [3]. While much effort has been devoted to investigating the influence of filler surface treatment on the rheological behavior of filled polymers, most studies have used commercial fillers such as carbon black, calcium carbonate, mica, and talc [5–7]. These fillers often have a complex structure and generally form aggregated suspensions with poorly characterized particle–matrix interactions impeding the interpretation of the rheological results.

The influence on melt rheology of model cross-linked fillers has been investigated by simple dispersion of the particles in different matrices [8–11], by incorporation of the particles into the matrix network through covalent bonding [12], and by adding a shell to enhance filler compatibility with the matrix [13–21].

In the current investigation, we sought to elucidate the rheological implications of particle–matrix interactions in a polyisoprene rubber matrix filled with low-density rubber-compatible model core-shell particles synthesized by a new method. The particles have a core derived from cross-linked polystyrene (PS) latex particles of uniform size, and a shell of terminally grafted PIP chains of uniform size. The new grafting path proposed is derived from an anionic *grafting onto* scheme we developed for the synthesis of arborescent polymers [22]. A significant disadvantage of the commonly used *grafting from* schemes – whereby the chains are grown from the surface of the particles – is that it is impossible to characterize the grafted chains unless they can be cleaved from the substrate. Under these conditions, the molecular weight of the side chains is typically approximated from linear chains grown in solution (e.g. due to residual initiator). The reactivity of initiating

* Corresponding author. Tel.: +1 519 888 4567; fax: +1 519 746 0435.
E-mail address: gauthier@uwaterloo.ca (M. Gauthier).

0032-3861/$ – see front matter © 2009 Elsevier Ltd. All rights reserved.
doi:10.1016/j.polymer.2009.10.050

sites located on a solid substrate can be significantly different from a free initiator however, so the size and polydispersity of the chains grown from the surface may also differ [23,24]. This problem is avoided in the *grafting onto* scheme proposed, since a sample of side chains can be removed from the reactor prior to grafting.

The synthesis of the model filler started from spherical PS latex particles of uniform size, cross-linked with 12 mol% divinylbenzene (DVB), obtained by starved-feed emulsifier-free emulsion polymerization [25]. The particles were functionalized by acetylation [22] and coupled with 'living' polyisoprenyllithium chains having a high 1,4-microstructure content and a uniform size ($M_w/M_n = 1.05–1.12$) as shown in Scheme 1 [22]. Two series of model filler samples were generated based on different acetylation levels for the latex particles, and PIP side chains having a number-average molecular weight $M_n = 1.5$ K, 5 K, or 30 K. A rubber matrix of linear polyisoprene (LPIP395, $M_n = 395$ K) with a high 1,4-microstructure content was blended with the model fillers. Freeze fracture scanning electron microscopy (SEM) was performed to characterize the degree of dispersion of the filler particles within the matrix. The rheological properties of the blends were then investigated to clarify the influence of particle–matrix interactions in term of the length and the weight fraction of the PIP chains in the filler on the frequency-dependent complex viscosity, storage modulus, and loss tangent curves. The addition of PIP chains on the surface of the particles provided control over the interactions between the filler and the rubber matrix. More favorable interactions should facilitate the dispersion of the filler and facilitate filler agglomerate break up under the influence of shear forces [26].

2. Experimental

2.1. Materials

Tetrahydrofuran (THF; Caledon, reagent grade) was purified by distillation from sodium-benzophenone ketyl under nitrogen. Cyclohexane (BDH, HPLC grade) was purified by refluxing with oligostyryllithium under nitrogen. The dry solvents were introduced directly from the purification stills into the polymerization reactor or ampule preparation manifolds through polytetrafluoroethylene (PTFE) tubing. Isoprene (Aldrich, 99%, inhibited with 100 ppm 4-*tert*-butylcatechol, TBC) was purified by distillation after stirring with CaH_2 overnight. Styrene (Aldrich, 99%, inhibited with 10–15 ppm TBC), and the cross-linker divinylbenzene (DVB, Aldrich, 55% meta and para isomers, 42% ethylvinylbenzene, and 3% diethylbenzene, inhibited with 1000 ppm TBC) were first washed in a separatory funnel with three aliquots of 2 M sodium hydroxide solution and with deionized water to remove the TBC. All monomers were stored at −20 °C until further use. Ammonium persulfate (Fisher), *n*-butyllithium (*n*-BuLi, Aldrich, 2.5 M in hexane), and *sec*-butyllithium (*sec*-BuLi, Aldrich, 1.3 M in cyclohexane) were used as received. The exact activity of the organolithium compound solutions was determined by the method of Lipton et al. [27]. 2,2′-Bipyridyl (Aldrich, 99+%) was dissolved in dry cyclohexane to give a 0.10 M solution. All other reagents were used as received from the suppliers. The reagent ampules used in the polymerization and grafting procedures were prepared by high-vacuum purification techniques and filled with dry nitrogen [28]. The ampules were equipped with PTFE stopcocks and ground glass joints for mounting on the polymerization reactor.

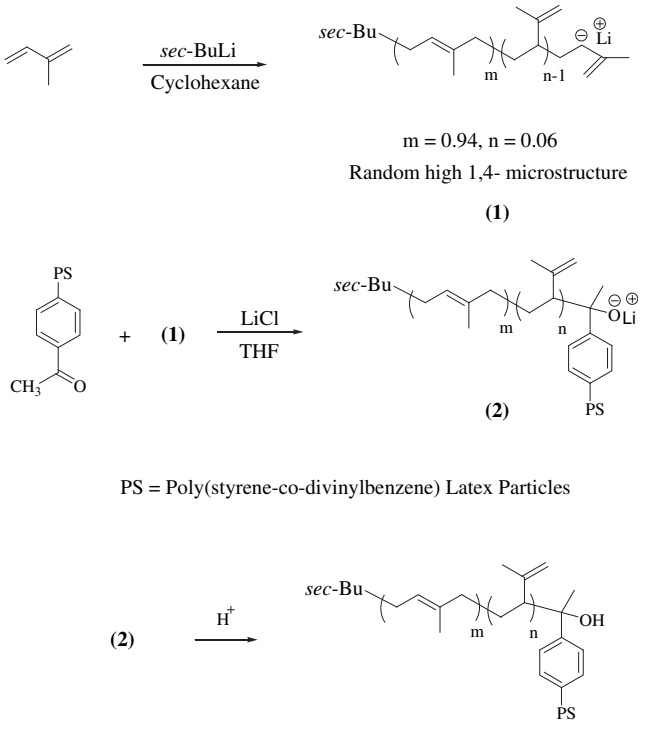

Scheme 1. Grafting of polyisoprenyllithium onto cross-linked acetylated polystyrene latex.

2.2. Synthesis of emulsifier-free poly(styrene-co-divinylbenzene) latex particles

Deionized water (1800 mL) was added to a 3-L resin kettle (glass reactor) immersed in a water bath at 70 ± 1 °C. Dissolved oxygen was chased from the reactor by bubbling nitrogen through the water for 60 min while stirring at 400 rpm. Purified styrene (80 mL, 0.70 mol) and DVB (6 mL, 0.04 mol) were then added to the reactor, which was left to stir for 20 min before adding ammonium persulfate (676 mg, 3.0 mmol, dissolved in 30 mL of deionized and deoxygenated water) to give a total initiator concentration of 1.64×10^{-3} M. Nucleation began (as indicated by an opalescent coloration) after 10 min and the reaction was allowed to proceed for 75 min. Nitrogen flow was continued throughout the reaction at a lower rate (ca. 1 bubble/s) to minimize evaporation. After the initial polymerization period, the addition of equal increments of a mixture of styrene and DVB in a volume ratio of 1:1 was started through a septum according to the addition scheme described in Table 1. There was a minimum of 20 min between each addition, to avoid pooling of monomer at the surface and destabilization of the emulsion. The reaction was allowed to proceed for a total of 8 h since the beginning of initiator addition. The particles were isolated by filtration over cheese cloth, flocculation of the aqueous latex with a minimum amount (ca. 10 mL) of concentrated (12 M) HCl, suction filtration, and drying under vacuum. Further purification of the particles involved their redispersion in THF, flocculation with a mixture of methanol and HCl (10:1 v/v), and drying under

Table 1
Addition sequence for styrene and DVB monomers in starved-feed system.

Time (min)	Volume DVB/Styrene (mL)
75	3.6
110	3.0
140	2.8
175	2.2
200	2.2
225	2.2
255	2.0
295	2.0

vacuum to constant weight. SEM analysis of the particles yielded a mean diameter $D = 400 \pm 6$ nm.

2.3. Acetylation of the latex particles

A sample of latex particles (64.0 g, 615 meq styrene units) was dried under vacuum in a 2-L round-bottomed flask and dispersed in 600 mL of nitrobenzene. For a target acetylation level of 30 mol%, a solution was prepared by dissolving anhydrous $AlCl_3$ (Aldrich, 99.99%, 27.0 g, 202 mmol) in 150 mL of nitrobenzene and adding acetyl chloride (16.0 mL, 225 mmol). The acetyl chloride–$AlCl_3$ solution was added dropwise to the particle dispersion over 60 min at room temperature (23 °C), and the reaction was allowed to proceed for 60 min. Product workup involved precipitation of the acetylated particles in 3 L of methanol acidified with 100 mL of concentrated (12 M) HCl, and recovery of the particles by suction filtration as a first step. Further purification was achieved by two cycles of redissolution in 200 mL of THF, precipitation in 2 L of methanol acidified with 40 mL of concentrated HCl, and suction filtration. The isolated particles were then redispersed in 200 mL of chloroform and precipitated one last time in 2 L of methanol, and recovered by suction filtration before drying under vacuum to constant weight. The same procedure was used for a target acetylation level of 5 mol%, by reducing the amount of reagents used (4.5 g, 34 mmol of $AlCl_3$ in 25 mL of nitrobenzene, and 2.7 mL, 37.5 mmol of acetyl chloride).

2.4. Synthesis of polyisoprene-grafted latex particles

Two series of grafted latex were generated from polystyrene particles with target acetylation levels (based on the reaction stoichiometry) of either 5 or 30 mol%, and side chains with $M_n = 1.5$ K, 5 K, or 30 K.

The polymerization of isoprene was performed in cyclohexane at room temperature, to obtain a microstructure with a high 1,4-units content. The synthesis from latex particles with a 30 mol% acetylation level and grafted with $M_n = 5$ K polyisoprene chains is provided as an example. The acetylated latex substrate (12 g, 30% acetylation, 31 mequiv acetyl units) was purified in an ampule by three cycles of azeotropic distillation with 100 mL of dry THF and redispersion in 100 mL of THF. Isoprene was further purified on a high-vacuum manifold immediately before polymerization by three freezing – evacuation – thawing cycles in the presence of *n*-BuLi solution (1 mL for 20 mL monomer) and slow distillation to a glass ampule. A five-neck 3-L glass reactor equipped with a mechanical stirrer was fitted with two ampules containing purified isoprene (54.5 g, 0.801 mol) and the acetylated latex substrate, dry THF and cyclohexane inlets, and a septum. Solid LiCl (2.31 g, 54.5 mmol) was loaded in the reactor before it was evacuated, flamed, and purged with purified nitrogen. Cyclohexane (500 mL) and 0.5 mL of 0.10 M 2,2′-bipyridyl solution were added to the reactor, and the solvent was titrated with the *sec*-BuLi solution to give a persistent light orange color [29]. The reactor was then cooled to 0 °C before the calculated amount of *sec*-BuLi (9.90 mL, 10.9 mmol, for a target $M_n = 5$ K) was added. The isoprene was added dropwise from the ampule and the reactor was warmed to room temperature after complete addition of the monomer. The polymerization was allowed to proceed for 5 h before cooling to 0 °C and adding 1 L of THF. A sample of the side chains was removed for characterization and terminated with degassed 2-propanol acidified with HCl. The reactor was cooled to −96 °C in a toluene/liquid nitrogen bath and the acetylated polystyrene latex particles dispersion was added at once. The reactor was warmed to room temperature (23 °C) in a water bath and stirred for 2 h, leading to complete fading of the color. The raw product (65 g) was recovered by precipitation in methanol and dried under vacuum. The grafted latex particles were isolated from linear PIP contaminant by redispersion of the raw product in hexane at a concentration of 10% by weight and centrifugation for 90 min at 6000 rpm. Successful purification was confirmed by the absence of a peak for the polyisoprene side chains in SEC analysis of the sample. The purified grafted particles (14.9 g) were recovered by redispersion in THF, precipitation in methanol, suction filtration, and drying under vacuum to constant weight.

2.5. Synthesis of linear polyisoprene

The polymerization of isoprene was performed in cyclohexane at room temperature to yield a microstructure with a high 1,4-unit content as before. The reaction used purified isoprene (185 g, 2.72 mol), dry cyclohexane (1.5 L), and *sec*-BuLi (0.96 mL) at room temperature (23 °C) for 72 h. After termination with 1 mL of degassed, acidified 2-propanol, the crude product (180 g) was recovered by precipitation in methanol and drying under vacuum for 24 h. The polymer had an absolute $M_n = 395\,000$ ($M_w/M_n = 1.09$), as determined by SEC analysis with a multi-angle laser light scattering (MALLS) detector, and a microstructure with 94% of 1,4-isoprene units (*cis*- and *trans*-isomers combined) and 6% of 3,4-units as determined by ^{1}H NMR spectroscopy analysis by the method of Tanaka et al. [30].

2.6. Blending

The polyisoprene-grafted latex particles and the linear polyisoprene used for the blends were stabilized by dissolution in THF with 0.25% w/w N-N′-diphenyl-1,4-phenylenediamine and evaporation to constant mass under vacuum over several days. Solution blending was achieved at room temperature (23 °C) by dispersing grafted latex particles and dissolving linear polyisoprene (LPIP395, 1.0 g) separately in 50 mL of THF with sonication for 60 min. Different amounts of grafted particles were used as reported in Table 2, depending on their polyisoprene weight fraction, so as to maintain a constant volume fraction $\phi_{PS} = 0.35$ for the polystyrene latex particles. After mixing, the two components were sonicated further for 30 min. The mixture was poured into a 150 mL PTFE beaker with a magnetic stirring bar and left to evaporate *with stirring* in a fume hood at room temperature, then dried further under vacuum, and stored at −78 °C.

2.7. Sample characterization

The size of the latex particles before and after grafting was assessed by SEM analysis. A drop of diluted latex in THF was evaporated on a SEM pin mount (aluminum stud), coated with gold

Table 2
Microstructure of the linear PIP matrix and chains grafted on the fillers, and composition of the blends.

Sample[a]	Microstructure/% 1,4-units	3,4-units	Blend composition[b] Grafted latex (g)
PS[5]-*g*-PIP1.5	88	12	0.68
PS[5]-*g*-PIP5	88	12	0.71
PS[5]-*g*-PIP30	94	6	0.46
PS[30]-*g*-PIP1.5	87	13	0.89
PS[30]-*g*-PIP5	88	12	0.90
PS[30]-*g*-PIP30	94	6	0.93
LPIP395	94	6	

[a] Sample nomenclature: For example, PS[5]-*g*-PIP1.5 refers to latex particles with a target acetylation level of 5 mol% grafted with $M_n = 1.5$ K polyisoprene side chains.
[b] Amount of grafted latex added to 1.00 g of LPIP395 to achieve a polystyrene core volume fraction $\phi_{PS} = 0.35$ in the blends.

in a Potaron sputter coater, and examined in a Hitachi S-570 scanning electron microscope with an acceleration voltage of 10–15 kV. The average diameter of the particles was calculated from a minimum sample of 20 particles, and the uncertainties reported correspond to the standard deviation on the measurements.

The morphology of the grafted latex particles was examined by TEM analysis on a Philips CM10 TEM instrument operating at 60 kV. Thin films were cast onto 400-mesh copper TEM grids coated with Formvar® and carbon (supplied by Electron Microscopy Sciences) by laying the grid on filter paper, acting as a wicking agent, and placing one drop of solution onto the grid using a pipette. The films were allowed to dry overnight in a Petri dish under ambient conditions. The solution concentrations used to cast the films ranged from 0.1 to 0.5% w/v (1–5 mg/mL).

The dispersion state of the particles within the blends was examined by freeze fracture SEM microscopy in the Department of Food Sciences, University of Guelph, Ontario. The samples were mounted on a copper holder designed for the Emscope SP2000A Cryo-preparation unit (Ashford, Kent, UK) using Tissue–Tek®, a cryo-mounting gel. The copper holders were immersed in liquid nitrogen slush (−207 °C), withdrawn from the freezing chamber under argon to prevent water condensation, and put under vacuum for fracturing to provide a fresh surface. The samples were coated with gold (30 nm) in the Emscope cryo-preparation system below −135 °C. The holder was then transferred with the frozen sample, onto the cold stage of the Hitachi S-570 SEM instrument while maintaining the temperature below −135 °C at all times. Digital SEM images were captured using the Quartz PCI imaging software (Quartz Imaging Corp., Vancouver, BC).

FT-IR spectroscopy served to monitor the acetylation reaction. Samples were prepared by sonication of 15 mg of latex particles in 5 mL of chloroform for 15 min, casting on a NaCl plate and slow drying under an inverted beaker. The spectra were recorded on a Perkin Elmer FT-IR instrument at a resolution of 4 cm^{-1} using 4 scans.

Routine SEC analysis was performed for the linear polyisoprene matrix sample, the polyisoprene side chains, the raw grafting products, and the purified grafting products on an instrument consisting of a Waters 510 HPLC pump, a Waters 410 differential refractometer (DRI) detector, and a Jordi 500 mm DVB linear mixed-bed column. The polymers were analyzed in THF at a flow rate of 1 mL/min. Since the signal from the MALLS detector (*vide infra*) was too weak for analysis, apparent M_w/M_n values for the 1.5 K PIP side chains were also obtained by analysis on the same instrument using a linear polystyrene standards calibration curve.

The absolute M_n and M_w/M_n of the linear polyisoprene matrix, the 5 K and the 30 K PIP side chains were determined by SEC-MALLS (multi-angle laser light scattering) analysis with a Wyatt Dawn DSP-F detector operating at 632.8 nm. The SEC-MALLS system used consisted in a Waters 590 programmable HPLC pump and Waters Ultrastyragel columns (10^4, 10^5, and 10^6 Å pore sizes) with THF at a flow rate of 1 mL/min. Polymer concentration measurements in the eluent were accomplished with a Waters 2410 DRI detector operating at 660 nm. The analysis was done with the Astra Version 4.70.07 software package.

^{1}H NMR spectroscopy served to determine the absolute M_n for the 1.5 K PIP side chain samples. The microstructure of the PIP linear matrix and side chains, and the composition of the grafted latex particles were also determined by ^{1}H NMR spectroscopy on a Bruker-300 (300 MHz) nuclear magnetic resonance spectrometer instrument in $CDCl_3$ at a concentration of 5%. The microstructure of the PIP samples was analyzed by the method of Tanaka et al. [30]. For the composition analysis of the grafted latex particles, ^{1}H NMR spectra were obtained by an internal standard method, by acquiring spectra under identical conditions for a known concentration of the purified particles, and then with a known amount of the PIP side chains. The area of the PIP peaks in the two samples was used to calculate the weight percentage of PIP in the product. The PIP contents were also determined gravimetrically from the yield of purified particles.

2.8. Rheology

The blends of linear polyisoprene and grafted latex particles were characterized on a Paar Physica US-200 Rheometer at 25 °C, using the parallel plate geometry (25 mm diameter, 1 mm plate gap). The blends were compression-molded at room temperature (23 °C) to ca. 1 mm thick × 25 mm diameter disks, loaded between the plates, and allowed to equilibrate for 1 h at 25 °C. Dynamic mechanical analysis (complex viscosity, storage modulus, and damping factor) was performed with a frequency sweep from 60 to 1×10^{-4} Hz at 25 °C. The strain amplitude was controlled at 15% for all the samples, following dynamic strain sweeps performed to determine the regime of linear viscoelasticity, using strains of 1–20% with different fixed frequencies (1, 10, 40, 60, and 80 Hz). Duplicate rheological measurements were obtained for ca. 1/3 of the samples and yielded similar results (±5–10% variation) in all cases.

3. Results and discussion

3.1. Emulsifier-free synthesis of poly(styrene-co-divinylbenzene) latex particles

Surfactants are commonly used in emulsion polymerization, to facilitate the emulsification of the monomer and to impart colloidal stability to the particles. This approach is problematic for certain applications such as in the current study, not only due to potential contamination of the blends by the surfactant, but also because of potential interference with the anionic grafting reaction. Consequently, surfactant-free emulsion polymerization was used to produce the cross-linked model fillers. In this approach the initiator concentration, solids content, temperature, and stirring rate must be carefully controlled to obtain stable emulsions [31]. These parameters also dictate the size and uniformity of the particles obtained. In the emulsifier-free method, the polar groups introduced as chain ends on the polymer stabilize the growing particles in the aqueous phase. The stabilizing surface groups for persulfate-initiated systems have been identified as a combination of sulfate, hydroxyl, and carboxyl functionalities, the proportion of each species depending on the exact reaction conditions [32].

The addition of a cross-linking agent (e.g. DVB) further complicates the polymerization procedure because it can destabilize the emulsion and lead to coagulation of the reaction. Commercial DVB is typically a mixture of the *para*- and *meta*-isomers. Both isomers have copolymerization reactivity ratios favoring the incorporation of DVB over styrene at the 12 mol% composition investigated ($r_1 = 0.260$, $r_2 = 1.18$ for styrene and *p*-divinylbenzene, respectively, and $r_1 = r_2 = 0.58$ for styrene and *m*-divinylbenzene, respectively). Simple combination of the two monomers in a batch polymerization reaction would result in non-homogenous cross-linking of the particles. For that reason, a starved-feed emulsifier-free emulsion polymerization technique [25] was preferred. The latex obtained had a solids content of 4.4% and a spherical shape (Fig. 1). The final solids content of the latex is somewhat lower than the theoretical value (5.56%). This can be explained by the loss of monomer (since N_2 bubbling was maintained throughout the reaction), but also by the formation of a small amount (4–5%) of coagulum. Distinct particles were observed in the SEM pictures after coagulation and redispersion of the product in a good solvent for polystyrene, as expected for cross-

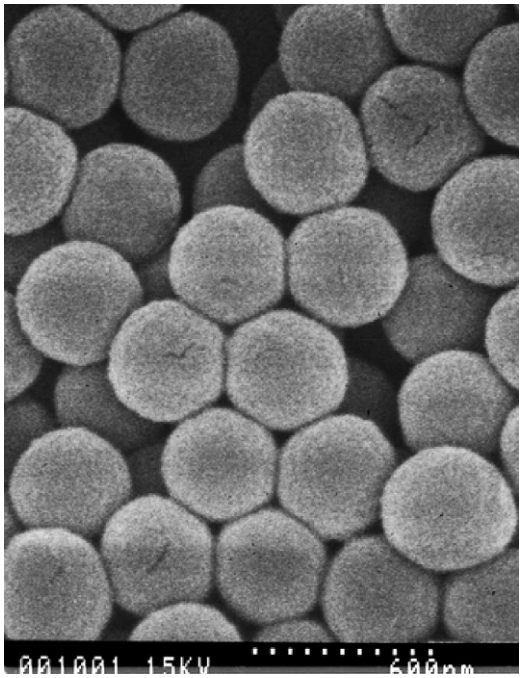

Fig. 1. SEM image for 400 nm spherical PS particles cross-linked with 12 mol% DVB.

linked particles. The particle diameter determined from the SEM images using the ImageJ 1.36b image processing and analysis program was 400 ± 6 nm. This substrate was used in the subsequent acetylation and grafting reactions.

3.2. Acetylation of poly(styrene-co-divinylbenzene) latex particles

Acetyl groups serving as coupling sites were incorporated in the latex particles by Friedel–Crafts acylation. The acetylation level attained is determined by nearly stoichiometric amounts of $AlCl_3$ and acetyl chloride [22]. Variation in the acetylation level thus provides control over the density of coupling sites on the substrate and the density of grafted polymer chains at the surface of the particles [33]. The target acetylation level was set at 5 mol% and 30 mol%, to obtain two different grafting site densities on the PS latex particles. While the acetylation level of linear polystyrene substrates can be conveniently quantified by ^{1}H NMR spectroscopy analysis [22], this method cannot be applied to the insoluble acetylated latex particles. Consequently, acetylation of the latex particles was rather confirmed qualitatively by FT-IR spectroscopy analysis, by the intense and well-resolved characteristic carbonyl stretching vibration at 1684 cm^{-1} (Fig. 2b) which is absent in the non-acetylated sample (Fig. 2a). The characteristic peak was much weaker for the substrate with a 5 mol% target acetylation level. Unfortunately, FT-IR analysis cannot provide accurate acetylation levels: It is not clear whether acetylation takes place evenly throughout the whole volume of the particles or preferentially on their surface, and the extent of penetration of the IR beam through the sample is unknown. This makes it impossible to use integrated absorbance peak intensity ratios for quantitative analysis. While it is clear that there is a difference in the concentration of acetyl coupling sites among the two substrates investigated (PS[5] vs. PS[30]), there is no reliable method to determine the density of acetyl groups directly at the surface of the particles. Depending on the relative rates of the acetylation reaction and the diffusion of the reagents within the cross-linked latex particles, it is possible that the acetylation reaction – in analogy to the grafting reaction – was limited to a layer close to the surface of the particles. In spite of this limitation, the presence of the absorbance peak at 1684 cm^{-1} can at least serve as indicative of the differing acetylation levels attained.

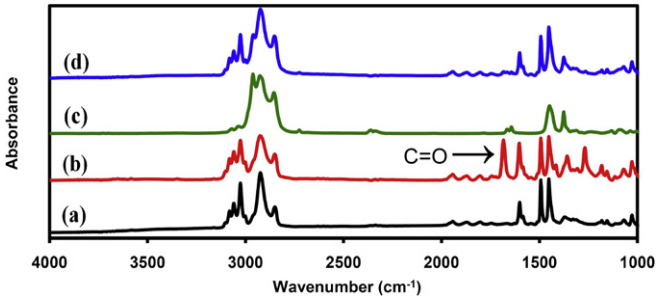

Fig. 2. FT-IR spectra for PS[30]-*g*-PIP5: (a) latex particles, (b) 30 mol% acetylated latex particles, (c) $M_n = 5$ K PIP side chains, and (d) grafted latex particles.

3.3. Polymerization of isoprene

The microstructure of polyisoprene chains is strongly dependent on the polarity of the solvent used [34] and, to a lesser extent, on the initiator and monomer concentrations in the reaction [35]. In non-polar (hydrocarbon) solvents a predominantly 1,4-microstructure resembling natural rubber is obtained, while more polar solvents (e.g. THF) lead to a mixed microstructure with high contents of 1,4-, 1,2-, and 3,4-isoprene units. For consistency, high 1,4-content polyisoprene chains were prepared for both the side chains grafted on the latex particles and the linear (matrix) PIP sample, by polymerization in cyclohexane.

The method for microstructure analysis [30] is based on the comparison of the area for the NMR peaks at 5.10 ppm (olefinic protons of the *cis*- and *trans*-1,4-units) and the doublet at 4.73 and 4.66 ppm (two vinylic protons of the 3,4-units). The results obtained for the analysis of the linear PIP sample and the side chain samples removed from the reactor prior to grafting are summarized in Table 2. The microstructure of the samples varied from 87 to 94% for *cis*- and *trans*-1,4-microstructures, and from 6 to 13 mol% for 3,4-units. The microstructure variations observed among the samples are consistent with the different initiator and monomer concentrations used in the polymerization reactions: An increase in initiator concentration or a decrease in monomer concentration should both lead to a decrease in 1,4-units content [34,35]. A lower 1,4-units content is indeed observed for shorter ($M_n = 1.5$ and 5 K) side chains, prepared at higher initiator concentrations and lower monomer concentrations than the $M_n = 30$ K side chains and the LPIP395 matrix polymer (Table 2).

3.4. Grafting reaction

The latex particles were grafted with polyisoprene side chains having a microstructure similar to the matrix polymer, to study the influence of filler particle–matrix interactions on the rheological behavior of the blends. The grafting reaction (Scheme 1) involves the nucleophilic addition of the macroanions on the acetyl coupling sites. This is best achieved in the presence of LiCl, to suppress chain end ionization and concomitant side reactions due to abstraction of the acidic acetyl protons terminating the macroanions.

The FT-IR spectrum for the 30% acetylated latex particles grafted with $M_n = 5$ K side chains, after removal of the linear PIP contaminant, is shown in Fig. 2d. The carbonyl stretch present at 1684 cm^{-1} for the acetylated latex particles (Fig. 2b) is negligible in the product, indicating the essentially complete consumption of the carbonyl groups by the polyisoprenyl anions in the reaction.

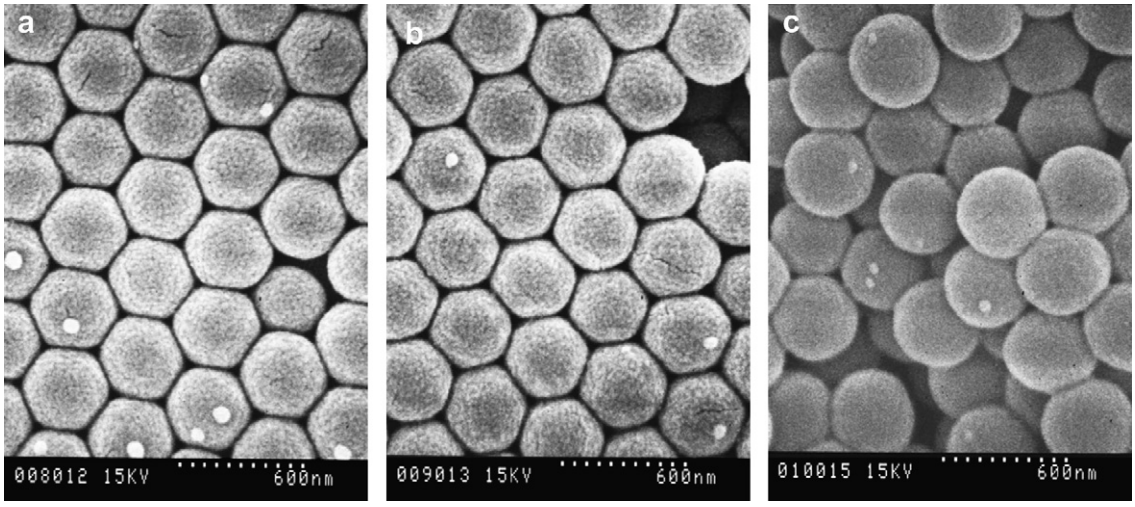

Fig. 3. SEM images for 5 mol% acetylated latex particles grafted with PIP: (a) PS[5]-*g*-PIP1.5, (b) PS[5]-*g*-PIP5, and (c) PS[5]-*g*-PIP30.

While the PIP side chains (Fig. 2c) have characteristic peaks mainly overlapping with those for the polystyrene latex substrate (Fig. 2a), and the PIP content of the grafted particles is modest (ca. 20% w/w), careful comparison of Fig. 2a and 2d reveals subtle differences in peak shape corresponding to the addition of the PIP component. SEM imaging (Figs. 3 and 4) shows the presence of smaller particles (secondary population), that are not visible in the original latex substrate (Fig. 1). Secondary populations normally form in emulsion polymerization due to active oligomers not captured by the existing particles [36]. Since these were not observed before acetylation of the latex, the exact origin of the smaller particles is not clear in the present case.

The characteristics of the grafted latex particles obtained are summarized in Table 3. Side chains with a high 1,4-isoprene units content were prepared by polymerization in cyclohexane, but a large volume of THF was introduced in the reactor to increase the polarity of the reaction mixture prior to grafting. This was done to increase the yield of the coupling reaction, found to be negatively influenced by low polarity solvents [37,38]. The grafting yield, defined as the fraction of side chains generated in the reaction that becomes coupled with the substrate, was determined from the relative peak areas in two successive SEC injections at identical concentrations for a pure PIP side chain sample and for the raw grafting product. Since only the linear contaminant was eluted from the SEC column, the grafting yield was calculated as the ratio of the peak area for the linear PIP component in the raw product over the peak area for the pure side chain sample. The grafting yield was found to decrease when grafting longer side chains onto the latex particles (Table 3). The inaccessibility to the macroanions of coupling sites buried within the substrate, and the presence of residual protic impurities difficult to remove from the rigid particle substrate, can explain in part the low (21–33%) grafting efficiencies obtained. Other factors potentially significant are the inherent immiscibility of the polystyrene and polyisoprene phases, and excluded volume effects due to chains already grafted on the surface of the particles hindering the diffusion of the macroanions to the coupling sites.

The thickness of the PIP shell (Table 3, column 5) was obtained by subtracting the core size (400 ± 6 nm) from the diameters determined from the SEM micrographs of Figs. 3 and 4 using the ImageJ 1.36b image processing and analysis program, using a minimum of 20 particles for the analysis. The shell thickness is ca. 25–30 nm and comparable for most samples, except for PS[5]-*g*-PIP1.5 and PS[5]-*g*-PIP5. The shell thickness obtained for these two samples is insignificant, considering the large standard deviations on the measurements. For composition analysis of the grafted latex

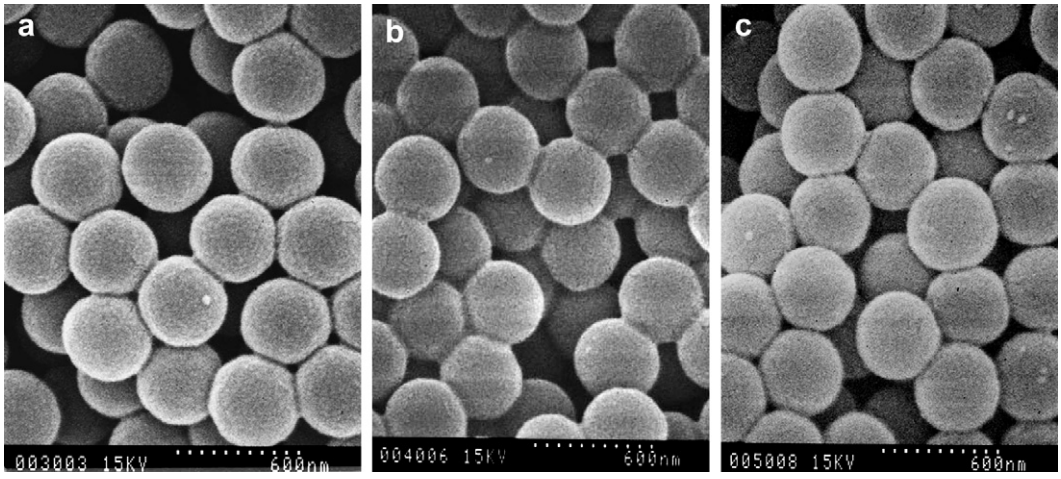

Fig. 4. SEM images for 30 mol% acetylated latex particles grafted with PIP: (a) PS[30]-*g*-PIP1.5, (b) PS[30]-*g*-PIP5, and (c) PS[30]-*g*-PIP30.

Table 3
Characteristics of polyisoprene-grafted latex particles and PIP side chains.

Sample	PIP side chains		PS[d] (g)	Graft PS			% w/w PIP		ϕ_{PS} Yield[j]
	M_n[c]	M_w/M_n[c]		Shell thick.[e] (nm)	Yield[f] (g)	Graft. eff. (%)[g]	NMR[h]	Yield[i]	
PS[5]-*g*-PIP1.5	1500[a]	1.08[b]	15	5 ± 21	15.9	33	–	5.66	0.93
PS[5]-*g*-PIP5	4900	1.09	15	4 ± 18	16.3	32	–	7.98	0.91
PS[5]-*g*-PIP30	26 800	1.12	15	27 ± 19	16.6	21	8.00	9.64	0.89
PS[30]-*g*-PIP1.5	1700[a]	1.10[b]	12	31 ± 14	14.8	31	5.50	18.9	0.79
PS[30]-*g*-PIP5	5400	1.05	12	24 ± 12	14.9	29	14.5	19.5	0.78
PS[30]-*g*-PIP30	28 600	1.12	14	29 ± 10	17.6	22	17.0	20.5	0.77

[a] M_n from ^{1}H NMR analysis.
[b] Apparent values from SEC analysis with a linear polystyrene standards calibration curve.
[c] Absolute values from SEC-MALLS analysis.
[d] Mass of acetylated latex particles used in the grafting reaction.
[e] Determined by SEM analysis.
[f] Yield of purified grafted particles.
[g] Fraction of side chains attached to the substrate.
[h] PIP content from ^{1}H NMR spectroscopy; no signal detected for PS[5]-*g*-PIP1.5 and PS[5]-*g*-PIP5.
[i] PIP content calculated from purified grafted particles yield.
[j] Volume fraction of polystyrene determined from the yield.

particles, ^{1}H NMR spectra were obtained under the same conditions for the fractionated particles (after the removal of non-grafted PIP chains) and after addition of a known amount of side chain material as an internal standard. Composition analysis of the grafted particles by ^{1}H NMR spectroscopy yielded polyisoprene contents varying from 5.5% to 17% by weight (Table 3, column 8). The polyisoprene contents were also estimated from the mass of particles isolated after the grafting reaction in comparison to the mass of the acetylated particles used (Table 3, column 9). The weight fraction of polyisoprene obtained by the two methods is significantly different. Analysis of the grafted particles by ^{1}H NMR spectroscopy, based on the peak area for the PIP chains, depends strongly on chain mobility. The PIP contents determined by that method are invariably lower than for the gravimetric method, in particular for shorter PIP chains. This deviation is attributed to the restricted mobility of the portion of the PIP chains attached to the particles, making these side chains difficult to detect by NMR spectroscopy. In fact no NMR signal was observed for particles grafted with very short ($M_n = 1.5$ K) PIP side chains, presumably for the same reason.

Evidence for a core-shell morphology was sought by TEM analysis of the bare and grafted particles. Comparison of the TEM pictures obtained (without staining) for the substrate with a 30% target acetylation level (Fig. 5a), and after grafting with $M_n = 5$ K PIP side chains (sample PS[30]-*g*-PIP5 purified to remove linear PIP contaminant, Fig. 5b), clearly shows the presence of interstitial material filling the gaps present between the bare particles. The presence of highly deformable chains in the shell of the grafted particles is consistent with a core-shell morphology.

3.5. Blending

It has been shown in the literature that blends of a linear polymer component and filler particles modified by grafting polymer chains having the same chemical composition and a molecular weight comparable with or greater than the matrix polymer are thermodynamically stable due to the suppression of depletion demixing [15,16,20]. This result is important from a fundamental viewpoint, but the composition of the systems used in these investigations bears little resemblance with practical filled polymer systems, including blends of a long chain polymer matrix and filler particles stabilized by short grafted chains. This problem was considered in other investigations, however [17,18,21,39]. It was likewise confirmed that a uniform distribution of grafted filler particles, and significant enhancements in tensile and rheological properties could be achieved under these conditions, as long as a minimum grafted chain length and surface grafting density were attained. The existence of an optimal surface grafting density maximizing the filler effects, and corresponding to complete coverage of the particle surface by the stabilizing chains in a coiled (rather than a brush) conformation, was also suggested [39]. The good filler dispersion observed in these systems was explained, in analogy to sterically stabilized dispersions, in terms of the excluded

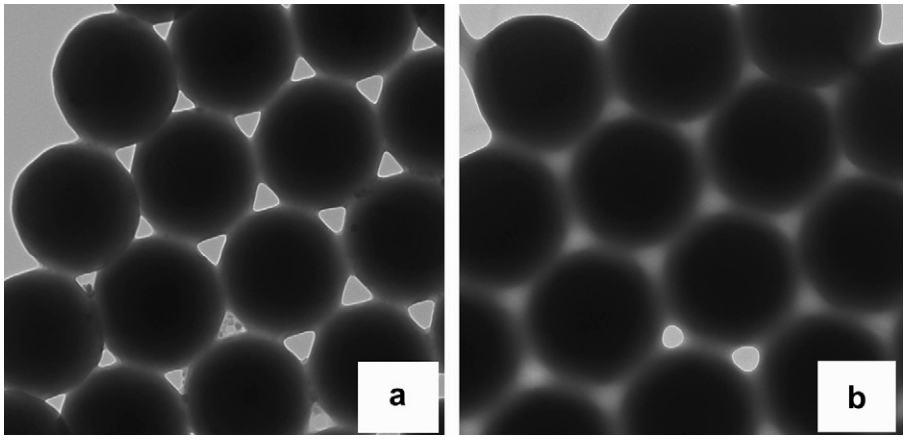

Fig. 5. TEM pictures for (a) bare latex particles with a 30% target acetylation level, and (b) grafted with $M_n = 5$ K PIP chains (sample PS[30]-*g*-PIP5).

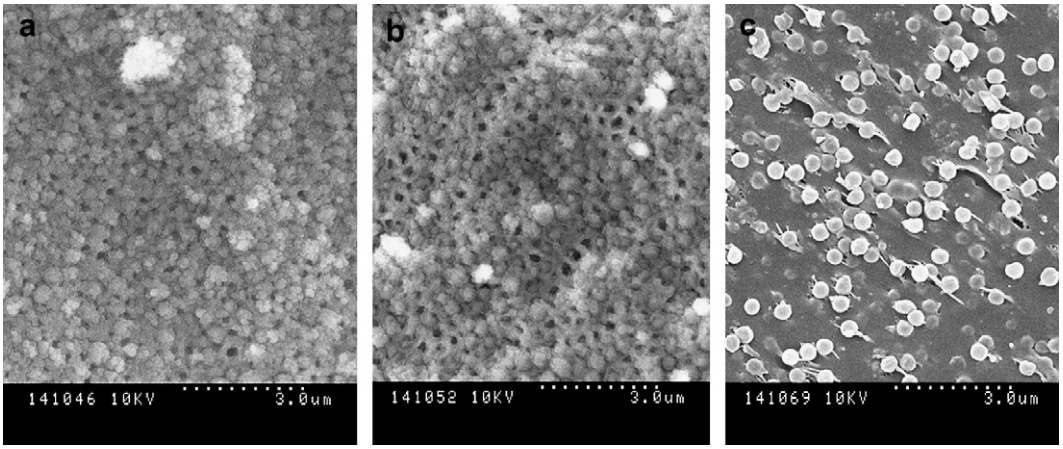

Fig. 6. SEM images for blends of 5 mol% acetylated particles grafted with PIP for (a) PS[5]-*g*-PIP1.5, (b) PS[5]-*g*-PIP5, and (c) PS[5]-*g*-PIP30.

volume effect of the coiled grafted chains opposing the van der Waals attraction potential between the particles [17]. It was also argued that entanglement formation between the grafted polymer and the matrix component should be possible in these filled polymers [17,21]. The experiments reported herein clearly belong to the second category, since the stabilizing chains grafted on the particles are short ($M_n = 1.5$–30 K) with respect to the linear PIP component ($M_n = 395$ K).

The composition of the blends investigated, provided in Table 2, was set to maintain a constant polystyrene core volume fraction $\phi_{PS} = 0.35$ after mixing with the LPIP395 matrix. The distribution of filler particles within the polyisoprene matrix was examined by the freeze fracture SEM technique. The SEM micrographs for the blends, provided in Figs. 6 and 7, show that even though some particle aggregation was present, the distribution of particles achieved within the matrix by solution blending was homogeneous.

It should be noted that while the particles are uniformly dispersed within the matrix polymer, the particles in the blend incorporating sample PS[30]-*g*-PIP30 (Fig. 7c) look significantly larger than in the other blends. This effect is attributed to enhanced entanglement of the grafted side chains with the matrix polymer leading to a larger effective particle volume. In contrast, no significant increase in apparent diameter (and presumably in entanglement level) is observed for blends based on the 5 mol% acetylated particles, even for $M_n = 30$ K side chains (Fig. 6c).

3.6. Rheology

Dynamic mechanical measurements were performed on the blends to study the influence of the polyisoprene side chain length and the composition of the particles on the viscoelastic properties of the filled polyisoprene matrix. To avoid complications such as cross-link density variations interfering with filler-related effects, the rheological properties of the blends were investigated without curing.

It is generally accepted that there is a strong correlation between the dispersion level of filler particles within a polymer matrix and the degree of mechanical property (e.g. modulus, tensile strength) enhancement observed. This was demonstrated for systems where the molecular weight of the chains grafted on the filler was comparable to or greater than the matrix polymer [15,16,20], as well as for systems where the grafted chains were shorter than the matrix polymer chains [17,18,21,39], even though the stabilization mechanism invoked differed in each case.

Two distinct regions are generally observed in modulus-frequency curves above the glass transition temperature (T_g) for linear, high molecular weight polymers [40]. These are visible for the linear polyisoprene matrix and for all the blends. The relatively flat plateau at high and intermediate frequencies is associated with localized motions of polymer segments restricted by entanglements. The low-frequency or terminal region is related to viscous flow (relaxation) of

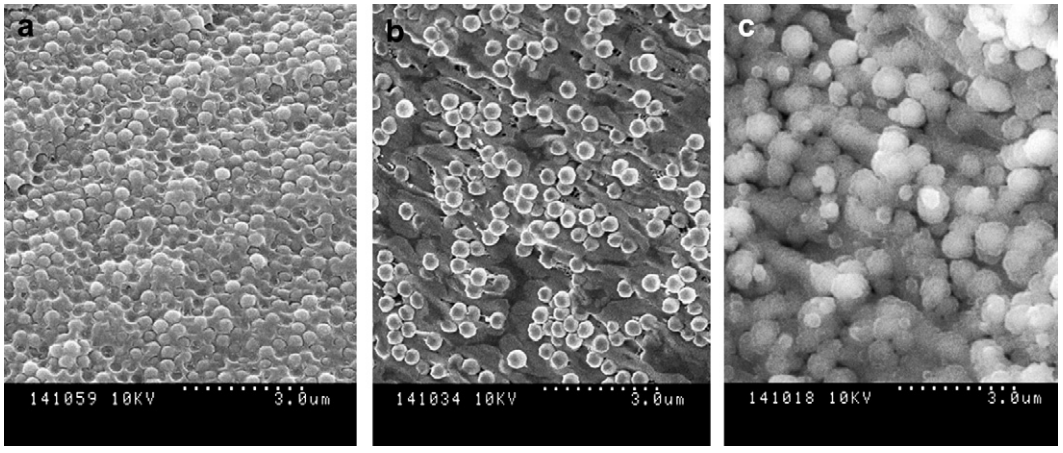

Fig. 7. SEM images for blends of 30 mol% acetylated particles grafted with PIP for (a) PS[30]-*g*-PIP1.5, (b) PS[30]-*g*-PIP5, and (c) PS[30]-*g*-PIP30.

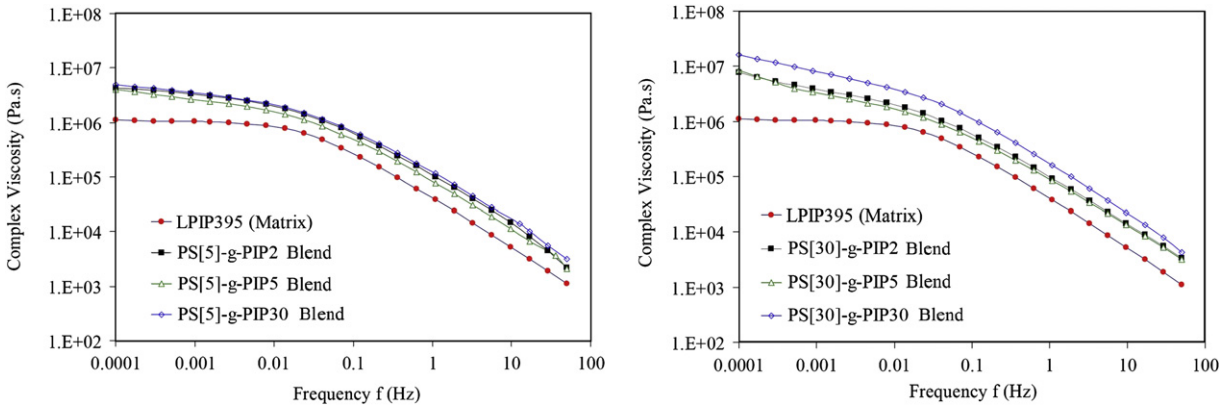

Fig. 8. Complex viscosity of LPIP395 matrix non-filled and filled with PS[5] (left) and PS[30] (right) particles grafted with polyisoprene side chains as indicated.

the polymer chains, involving motions of the entire molecules. This terminal relaxation process is most effectively described by reptation motions of a chain along its entangled length [41].

The rheology of filled polymers has been shown to depend on the structure and the composition of the filler and the matrix, because of variations in the particle–matrix interactions. It was thus suggested that strong interactions tend to increase the viscosity and the dynamic modulus, as polymer chains bonded or adsorbed onto the filler surface restrict the mobility of the matrix polymer chains [3,4]. A number of investigations indeed reported significant increases in viscosity and dynamic modulus after the surface treatment of fillers with a binding or coupling agent to increase the interactions between the polymer matrix and the fillers [12,13,42–44]. Dynamic mechanical measurements were also performed on blends of a low molecular weight polysulfide matrix with fillers of different chemical compositions [11]. In this case, the authors argued that fillers which were "chemically compatible" with the matrix due to better particle–matrix interactions were better dispersed within the matrix, and led to larger increases in dynamic modulus and viscosity. In the case of polymer-grafted filler particles similar arguments have been invoked in relation to the surface tension between the particles and the matrix, but entanglement formation between the grafted chains and the polymer matrix must also be considered [17,21]. On the basis of these trends a similar influence of the grafted PIP chains was expected, due to variations in the degree of compatibilization and entanglement of the particles with the PIP matrix.

The complex viscosity (η^*), storage modulus (G'), and damping factor (tan δ) curves, obtained for the blends as a function of frequency from 1×10^{-4} to 60 Hz, are shown in Figs. 8–10, respectively. It is clear that the rheology of the polymer matrix is significantly affected by the grafted particles. Some degree of compatibilization of the filler particles was obviously achieved, and presumably entanglement between the grafted and the matrix chains. The grafted polyisoprene shell increases the complex viscosity and the storage modulus for all the blends in the high frequency range (1–60 Hz), corresponding to the plateau region of the modulus curves, as well as in the low frequency range (10^{-4}–1 Hz), related to chain relaxation. The increases are more important for particles based on a target acetylation level of 30 mol%, containing a larger number of compatibilizing polyisoprene chains at their surface, than for particles based on an acetylation level of 5 mol% (Figs. 8 and 9). For sample PS[30]-*g*-PIP30 (Fig. 9), the storage modulus of the blend is almost 4-fold larger than for the non-filled LPIP395 matrix in the rubbery plateau region (ca. 0.1–50 Hz), in good agreement with the 3.6-fold increase predicted by the Guth–Smallwood equation [45], $G = G_0\ (1 + 2.5\ \phi + 14.1\ \phi^2)$, where G, G_0, and $\phi = 0.35$ represent the modulus of the filled polymer, the modulus of the non-filled polymer matrix, and the volume fraction of the filler, respectively. In comparison, samples PS[30]-*g*-PIP1.5 and PS[30]-*g*-PIP5 displayed somewhat lower increases in the rubbery plateau region, i.e. 2.3-fold and 2.5-fold, respectively. For samples PS[5]-*g*-PIP1.5, PS[5]-*g*-PIP5, and PS[5]-*g*-PIP30, based on 5 mol% acetylated particles, the rubbery modulus of the blends is 2.7-fold, 2.0-fold, and 3.0-fold larger than for the non-filled LPIP395 matrix, respectively (Fig. 9). In all cases, the modulus increases are well above the variations observed in duplicate rheological measurements (±5–10%). Since the particles were shown to be uniformly distributed in all the blends, this effect is attributed to a higher degree of entanglement for the longer ($M_n = 30$ K) polyisoprene side chains with the matrix. This should increase the frictional resistance of the polymer chains, and thus

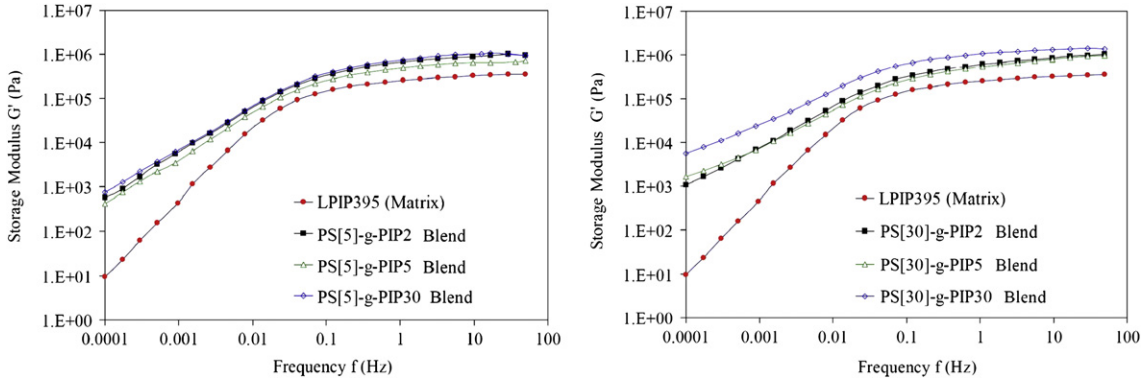

Fig. 9. Storage modulus of LPIP395 matrix non-filled and filled with PS[5] (left) and PS[30] (right) particles grafted with polyisoprene side chains as indicated.

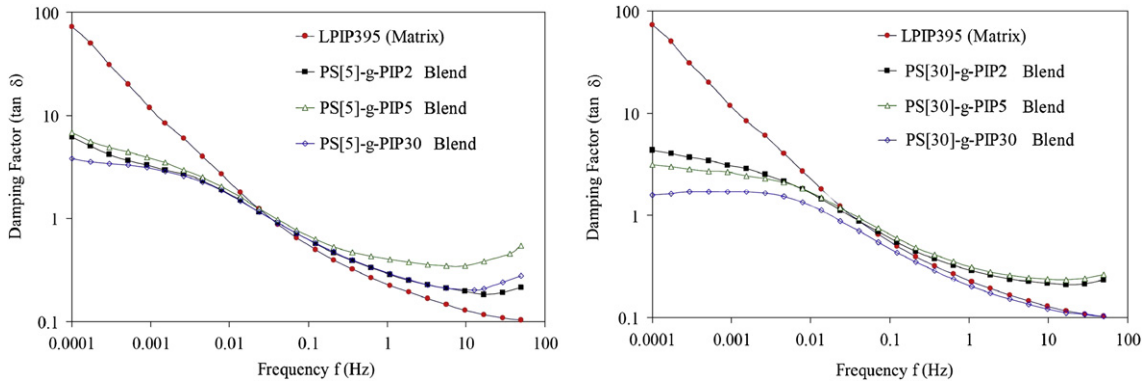

Fig. 10. Damping factor of LPIP395 matrix non-filled and filled with PS[5] (left) and PS[30] (right) particles grafted with polyisoprene side chains as indicated.

the viscosity of the blends. A similar mechanism was suggested to explain the behavior of carbon black-filled rubbers for which filler–matrix interactions dominated [2]. Another study suggested an identical mechanism to explain the behavior of SBR filled with core-shell particles (PMMA core and polystyrene shell) and carbon black, by showing that the interactions of the matrix with the core-shell particles dominated over those with carbon black [13].

Furthermore, it is interesting to note that while multiple relaxations have been observed for thermodynamically stable blends of low molecular weight matrices and filler particles modified with long side chains [16], these are not observed in the current investigation. Apart from the increased rubbery modulus, attributed to a classical filler effect, the only significant change observed for the filled polymer samples is delayed terminal flow. This effect, more significant for filler particles with longer stabilizing chains (M_n 30 K > 5 K ≈ 1.5 K) and a higher grafting density (PS[30] > PS[5]) is consistent with enhanced entanglement formation with the linear polymer matrix.

The ratio of the loss and storage moduli (G''/G'), also called the damping factor or tan δ, corresponds to the ratio of energy dissipated to energy stored in a deformation cycle. At high frequencies (~1–60 Hz) the PIP matrix and all blends are within the rubbery plateau region, where energy storage and loss are determined by the local motions of the polymer chain segments. Since the relaxation time for the rigid filler particles is much longer than for the chain segments in the matrix, tan δ is determined mainly by the PIP matrix and is not strongly affected by the filler particles. Consequently, tan δ appears to be relatively insensitive to blend composition over that frequency range. In the low frequency range (~0.0001–0.1 Hz), since the whole polymer molecules can move, the non-filled PIP matrix behaves like a viscous liquid and tan δ increases. Comparatively lower tan δ values are observed for all the blends in the low frequency range (Fig. 10), the change being most prominent for particles based on 30 mol% acetylation. This result suggests that favorable particle–matrix interactions due to the grafted shell of polyisoprene chains increase the elasticity of the blends. The high density of grafted PIP chains on the particles favors chain entanglement and the formation of an elastic network with the PIP matrix chains that restricts the flow of the whole molecules. Indeed, the largest decreases in tan δ are observed for the blends of the particles grafted with longer PIP chains (M_n = 30 K), presumably due to their more extensive entanglement with the matrix chains.

4. Conclusions

Monodispersed polystyrene latex particles cross-linked with 12 mol% DVB were prepared by starved-feed emulsion polymerization in the absence of emulsifier. The particles obtained were of uniform, spherical shape with a diameter of 400 ± 6 nm as determined by SEM analysis. Activation of the particles was achieved by acetylation to target levels of 5 mol% and 30 mol% prior to grafting with 1,4-polyisoprene side chains with a molecular weight of either 1500, 5000, or 30 000. The weight fraction of polyisoprene in the grafted particles was determined from the recovery yield of purified product and by NMR spectroscopy. Freeze fracture SEM imaging of blends of the linear PIP with the modified filler particles confirmed that the particles were uniformly distributed within the polyisoprene matrix in most cases.

The influence of filler structure on the rheological behavior of the blends was examined by dynamic mechanical analysis in terms of frequency-dependent complex viscosity, storage modulus, and damping factors over a frequency range of 10^{-4}–60 Hz. All the blends exhibited enhanced complex viscosity, storage modulus, and decreased damping factor values relative to the matrix polymer. On that basis, it appears that the interactions between the filler particles and the polymer matrix decreased in the order 30 mol% > 5 mol% acetylation, and in terms of the M_n of the grafted PIP chain length, 30 000 > 5000 ≈ 1500. The tan δ of the blends appears to be relatively insensitive to filler composition in the rubbery plateau (~1–60 Hz) region, but it is lower in comparison to the non-filled polymer matrix in the low-frequency (flow) region. The decreased damping factors, indicative of lower heat dissipation, could be interesting for applications where the generation of heat is undesirable such as tires.

Acknowledgements

The financial support of the Natural Sciences and Engineering Research Council of Canada (NSERC) is gratefully acknowledged. We thank Prof. Neil McManus, Department of Chemical Engineering, University of Waterloo, for the use of the SEC-MALLS equipment, and Dr. Sandy Smith, Department of Food Sciences, University of Guelph, for running the freeze fracture SEM measurements.

References

[1] Byers JT, Wayner MP. In: Morton M, editor. Rubber technology. 3rd ed. New York: Van Nostrand Reinhold; 1987 [chapter 3].
[2] Wolff S, Wang M-J. Rubber Chem Technol 1992;65:329–42.
[3] Agarwal S, Salovey R. Polym Eng Sci 1995;35:1241–51.
[4] Zhu J, Ou Y-C, Feng Y-P. Polym Int 1995;37:105–11.
[5] Metzner AB. J Rheol 1985;29:739–75.
[6] Kamal MR, Mutel A. J Polym Eng 1985;5:293–382.
[7] Yilmazer U, Farris RJ. J Appl Polym Sci 1983;28:3369–86.
[8] Park M, Gandhi K, Sun L, Salovey R, Aklonis JJ. Polym Eng Sci 1990;30:1158–64.

[9] (a) Sun L, Park M, Salovey R, Aklonis JJ. Polym Eng Sci 1992;32:777–85;
(b) Sun L, Park M, Aklonis JJ, Salovey R. Polym Eng Sci 1992;32:1418–25.
[10] Sun L, Aklonis JJ, Salovey R. Polym Eng Sci 1993;33:1308–19.
[11] Cai JJ, Salovey R. J Polym Sci Part B Polym Phys 1999;37:815–24.
[12] Nuyken O, Bayer R. Kautsch Gummi Kunstst 1995;48:704–8.
[13] Nuyken O, Ko S-K, Voit B, Yang D. Kautsch Gummi Kunstst 1995;48:784–7.
[14] (a) Merrington A, Yang Z, Meier DJ. In: Proc. 1st Int. Particle Technol Forum Amer Inst Chem Eng; 1994.
(b) Yang Z, Merrington A, Meier DJ. Polym Mater Sci Eng 1995;73:438–9.
[15] Lindenblatt G, Schärtl W, Pakula T, Schmidt M. Macromolecules 2000;33:9340–7.
[16] Lindenblatt G, Schärtl W, Pakula T, Schmidt M. Macromolecules 2001;34:1730–6.
[17] Zheng L, Feng Xie A, Lean JT. Macromolecules 2004;37:9954–62.
[18] Wang X, Hall JE, Warren S, Krom J, Magistrelli JM, Rackaitis M, et al. Macromolecules 2007;40:499–508.
[19] Shi L, Bi W, Chen H, Tang T. J Polym Sci Part A Polym Chem 2007;45:4477–86.
[20] Wang X, Foltz VJ, Rackaitis M, Böhm GGA. Polymer 2008;49:5683–91.
[21] Jakuczek L, Gutmann JS, Herrmann C, Żuchowska D. Polimery 2008;53:888–92.
[22] Li J, Gauthier M. Macromolecules 2001;34:8918–24.
[23] Zhou Q, Wang S, Fan X, Advincula R, Mays J. Langmuir 2002;18:3324–31.
[24] Zhou Q, Fan X, Xia C, Mays J, Advincula R. Chem Mater 2001;13:2465–7.
[25] Ding ZY, Ma S, Kriz D, Aklonis JJ, Salovey R. J Polym Sci Part B Polym Phys 1992;30:1189–94.
[26] Todd DB. Adv Polym Tech 2000;19:54–64.
[27] Lipton MF, Sorensen CM, Sadler AC, Shapiro RH. J Org Chem 1980;186:155–8.
[28] Gauthier M, Tichagwa L, Downey JS, Gao S. Macromolecules 1996;29:519–27.
[29] Liu W-L, Loveless FC. U.S. Patent 5 489 649; 1996.
[30] Tanaka Y, Takeuchi Y, Kobayashi M, Tadokoro H. J Polym Sci Part A-2 Polym Phys 1971;9:43–57.
[31] See for example Shouldice GTD, Vandezande GA. Rudin A Eur Polym J 1994;30:179–83.
[32] Goodwin JW, Hearn J, Ho CC, Ottewill RH. Br Polym J 1973;5:347–62.
[33] Gauthier M, Möller M, Burchard W. Macromol Symp 1994;77:43–9.
[34] Worsfold DJ, Bywater S. Can J Chem 1964;42:2884–92.
[35] Worsfold DJ, Bywater S. Macromolecules 1978;11:582–6.
[36] (a) Morrison BR, Gilbert RG. Macromol Symp 1995;92:13–30;
(b) Stutman DR, Klein A, El-Aasser SM, Vanderhoff JW. Ind Eng Chem Prod Res Dev 1985;24:404–12.
[37] (a) Takaki M, Asami R, Ichikawa M. Macromolecules 1977;10:850–5;
(b) Takaki M, Asami R, Kuwata Y. Polym J 1979;11:425–8.
[38] (a) Kee RA, Gauthier M. Macromolecules 1999;32:6478–84;
(b) Li J, Gauthier M, Teertstra SJ, Xu H, Sheiko SS. Macromolecules 2004;37:795–802.
[39] Hasegawa R, Aoki Y, Doi M. Macromolecules 1996;29:6656–62.
[40] Ferry JD. In: Viscoelastic properties of polymers. 3rd ed. New York: Wiley; 1980. p. 267.
[41] Graessley WW. Adv Polym Sci 1982;47:67–117.
[42] Bretas RES, Powell RL. Rheol Acta 1985;24:69–74.
[43] Chiu W-Y, Hsueh TC. J Appl Polym Sci 1986;32:4663–78.
[44] Scherbakoff N, Ishida H. Polym Mater Sci Eng 1991;65:337–8.
[45] (a) Smallwood HM. J Appl Phys 1944;15:758–66;
(b) Guth E. J Appl Phys 1945;16:20–5.